Article

Peptide Nucleic Acids Containing Cationic/Amino-Alkyl Modified Bases Promote Enhanced Hybridization Kinetics and Thermodynamics with Single-Strand DNA

Frank Podlaski,[#] Stephen Cornwell,[#] Kenny Wong, Brian McKittrick, Jae-Hun Kim, Daram Jung, Yeasel Jeon, Kwang-Bok Jung, Peter Tolias, and William T. Windsor*

Cite This: ACS Omega 2023, 8, 33426−33436

Read Online

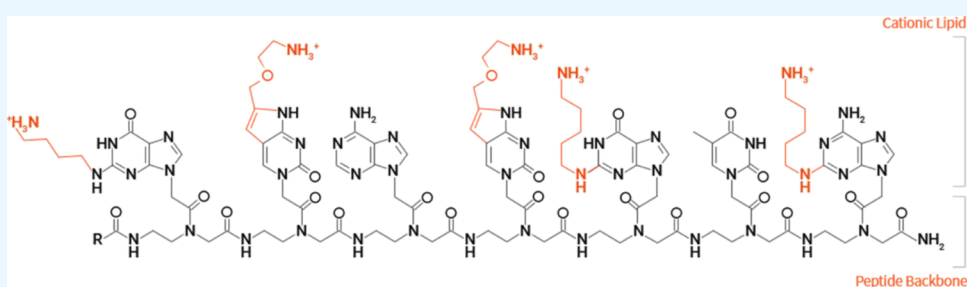| ACCESS | 📊 Metrics & More | 📖 Article Recommendations | ⓢ Supporting Information |

ABSTRACT: Peptide nucleic acids (PNAs) are antisense molecules with excellent polynucleotide hybridization properties; they are resistant to nuclease degradation but often have poor cell permeability leading to moderate cellular activity and limited clinical results. The addition of cationic substitutions (positive charges) to PNA molecules greatly increases cell permeability. In this report, we describe the synthesis and polynucleotide hybridization properties of a novel cationic/amino-alkyl nucleotide base-modified PNA (OPNA). This study was designed to quantitate the effect the cationic/amino-alkyl nucleotide base modification had on the kinetic and thermodynamic properties of OPNA-DNA hybridization using surface plasmon resonance and UV thermal melt studies. Kinetic studies reveal a favorable 10−30 fold increase in affinity for a single cationic modification on the base of an adenine, cytosine, or guanidine OPNA sequence compared to the nonmodified PNA strand. The increase in affinity is correlated directly with a favorable decrease in the dissociation rate constant and increase in the association rate constant. Introducing additional amino-alkyl base modifications further favors a decrease in the dissociation rate (3−10-fold per amino-alkyl). The thermodynamics driving the OPNA hybridization is promoted by an additional favorable −80 kJ/mol enthalpy of binding for a single amino-alkyl modification compared to the PNA strand. This increase in enthalpy is consistent with an ion−ion interaction with the DNA strand. These kinetic and thermodynamic hybridization studies reveal for the first time that this type of cationic/amino-alkyl base-modified PNA has favorable hybridization properties suitable for development as an antisense oligomer.

INTRODUCTION

Antisense oligonucleotides (ASO) are nucleotide polymers that bind to complementary sequences of RNA or DNA oligonucleotides. Antisense oligonucleotides (ASOs) have been used to successfully treat a wide range of muscular, neurological, immunological, eye, and metabolic diseases and disorders.[1,2] The mechanism of action for these disease modifiers includes the stimulation of RNA degradation by RNAse H1, modification(alteration) of pre-mRNA splicing to mature mRNA and immune stimulation by recruiting proteins to regulator sites.[2,3] The successful clinical application of the ASO strategy has been mediated by the design of novel modifications to the oligonucleotides to provide enhanced metabolic stability, increased affinity to targeted nucleotide sequences, and cell permeability.[4,5] One of the earlier methods to prevent enzymatic degradation of these typically short oligonucleotides (10−20 base pairs) was to replace the phosphate ribose backbone with a peptide backbone which utilizes a modified N-(2-aminoethyl)glycine peptide backbone and attached nucleotide bases without the sugar component.[4,6−11] While these peptide nucleic acids (PNA) have excellent nucleotide hybridization properties, are resistant to nuclease degradation, and are used extensively in diagnostics and as probes, they have poor cell permeability and fast clearance from the body and thus requires high concentrations in both cell-based and in vivo models to observe effects on
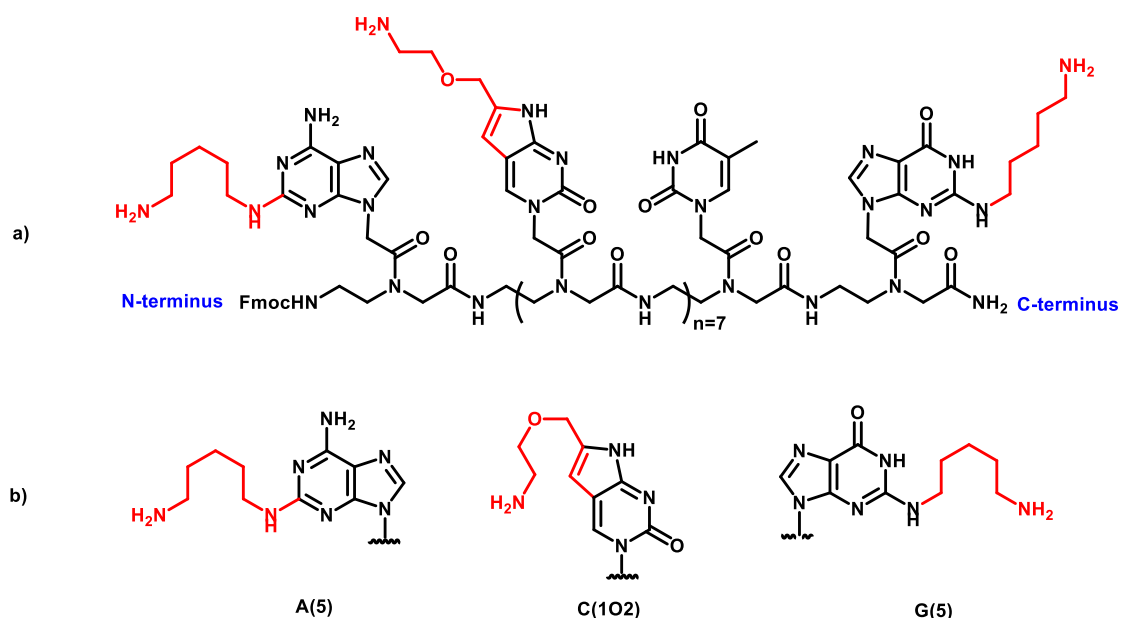
Figure 1. (a) Generic structure of a 10mer OPNA with modified bases and (b) chemical structure of each modified base.

target levels and function.[12−14] To improve cell-permeability, several strategies have been employed including formulating/ encapsulating the antisense PNA with phospholipids as well as introducing additional chemical modifications on the peptide backbone such as adding positively charged groups like lysine and arginine amino acids or G-clamps to the synthetic oligonucleotide.[4,5,9−11,15−19] This study will describe another strategy to improve cell permeability through the introduction of cationic/amino-alkyl positive charges directly on the PNA nucleotide bases (this type of ssPNA is referred to as OliPass PNA or OPNA).[20−24] Data suggest that these OPNA ASO have enhanced cell permeability and cell-based activity without the use of permeability agents such as transfection reagents or phospholipids.[20−25] Phase 1 and phase 2 clinical trials are ongoing to evaluate the efficacy of OPNA antisense molecules.[26−28] This report provides information regarding the synthesis and the kinetic and thermodynamics of the OPNA-DNA hybridization process which may provide insight into some of the cellular activities of OPNA (e.g., gene silencing and modulating the processing of pre-mRNA into mRNA).

Selection of optimal synthetic single strand ASO oligonucleotides requires studying many different molecules in in vitro assays that measure affinity, stability, and cellular responses, in addition to in vivo models. Cell-based assays and in vivo models vary greatly depending on the intended target and desired disease outcome. However, the analytical methods for characterizing the thermodynamic, kinetic, and thermal stability of oligonucleotide hybridization are performed by only a few different types of methods. The techniques and signals most often used include UV thermal melt assays, time-dependent fluorescence enhancement or quenching, and surface plasmon resonance (SPR).[29−36] In this current report, we have used SPR to measure the hybridization kinetics of short 8−10mer single-strand OPNA oligomers to a conserved biotin-immobilized complementary ssDNA. Experiments were designed to study the effect different amino-alkyl-base modifications would have on the kinetics and thermodynamics that promotes hybridization to provide insight into the optimal

design of OPNA oligomers. From temperature-dependent kinetics of OPNA-DNA hybridization, it is apparent that dimerization for the short ASO strands is consistent with a two-state model, indicating that the selected amino-alkyl-base modifications do not form undesirable structures that would hinder binding and lead to non-2-state binding (see general 2-state review: Ouldridge et al., 2013).[37] The enhanced affinity of OPNA vs a nonmodified PNA is driven greatly by the amino-alkyl-base mediated decrease in the dissociation rate. Finally, from temperature-dependent kinetic studies, thermo-dynamic analysis provided enthalpy of binding, ΔH, and entropy of binding, ΔS, values. These results indicate the addition of 1 cationic/amino-alkyl-base modification to an OPNA adenine, cytosine, or guanine enhanced the ΔH of binding by approximately −80 kJ/mol, indicating that the base modifications not only facilitates cell permeability but also promotes new and favorable molecular interactions that stabilize the OPNA-DNA double strand. The favorable kinetic and thermodynamic results presented in this report suggest that OPNA have properties that will favor their application as ASO in a wide range of diseases.

■ MATERIAL AND METHODS

DNA Oligonucleotide for SPR. Sense and antisense single strand DNA oligonucleotides were synthesized by Integrated DNA Technologies (Coralville, IA). Immobilized sense strands were labeled with biotin at the 5′ end. All oligonucleotides were HPLC-purified, confirmed by mass spectroscopy, and suspended in deionized water to make a working 500 μM stock. Each of the 5′-biotin sense strands were designed to have the OPNA 10mer bases bind to a 12mer DNA sequence where a single nonsense base was added to the 3′ and 5′ ends, leading to hybridization only to the central complementary 10 bases. This design was intended to decrease steric hindrance upon binding to the immobilized biotin/streptavidin sensor as well as provide symmetry for binding. The 10mer ssDNA antisense sequence control that corresponds to the 10mer OPNA antisense sequence is 3′-GTAGATCACT-5′.

Table 1. Nucleotide Sequences of Antisense Strands Used in Kinetic Study[a]

Oligonucleotide	Sequence										Tm (°C)
OPNA-0	5'-Fmoc-G	T	A	G	A	T	C	A	C	T-NH2	51
OPNA-1A	5'-Fmoc-G	T	A	G	**A(5)**	T	C	A	C	T-NH2	55
OPNA-1G	5'-Fmoc-G	T	A	**G(5)**	A	T	C	A	C	T-NH2	53
OPNA-1C	5'-Fmoc-G	T	A	G	A	T	**C(1O2)**	A	C	T-NH2	59
OPNA-2A	5'-Fmoc-G	T	**A(5)**	G	A	T	C	**A(5)**	C	T-NH2	61
OPNA-3A	5'-Fmoc-G	T	**A(5)**	G	**A(5)**	T	C	**A(5)**	C	T-NH2	66
OPNA-2A1C	5'-Fmoc-G	T	**A(5)**	G	**A(5)**	T	**C(1O2)**	A	C	T-NH2	69

[a]Bold: OPNA modification sites, modification types in parenthesis. [b]Thermal melting temperature: T_m.

OPNA Synthesis. OPNAs were produced by OliPass Corporation as 10mer peptide nucleic acids complementarily binding a 10mer DNA sequence. The sequence of the oligonucleotide was chosen for experimental exploration and not intended to have a genetic correlation. In brief, OPNAs were synthesized by solid phase peptide synthesis (SPPS) on an automatic peptide synthesizer (Tribute, Protein Technologies Inc) by Fmoc-chemistry based on the method disclosed in a patent disclosure.[38] H-Rink Amide ChemMatrix resin was purchased from PCAS BioMatrix Inc. (Quebec, Canada) and was used as a solid support. After synthesis, each OPNA was purified by C18-reverse phase HPLC (water/acetonitrile with 0.1% TFA) and identified using high-resolution mass spectrometry. A detailed OPNA synthetic procedure is described in the Supporting Information. The 10mer OPNAs used in this experiment are PNA oligomers possessing the general oligomer structural features, as shown in Figure 1A. OPNA oligomers were synthesized with natural nucleotide bases (A, G, C, and T) and unnatural amino-alkyl modified nucleobases having a primary amine group. Three unnatural modified nucleobases A(5), C(1O2), and G(5) used in this study are shown in Figure 1B. Figure 1B shows the structure of the basic OPNA monomer unit. The OPNA sequences used in this study are described in Table 1, for example, as [(N → C) Fmoc-GTA(5)GA(5)TC(1O2)ACT-NH₂] for OPNA-2A1C, wherein the PNA monomers marked with parenthesis are the monomers with an unnatural nucleobase having a basic primary alkyl amine group covalently tethered. OPNA are N-term-protected with Fmoc to prevent possible intramolecular cyclization leading to truncated OPNA. The calculated and observed molecular weights are shown in Supplementary Table S4.

Modified OPNA Monomer Synthesis. A(5), C(1O2), and G(5) synthesis are described in the Supporting Information.

Surface Plasmon Resonance Kinetics and Analysis. All SPR experiments were carried out using a Sartorius Pioneer FE (Sartorius BioAnalytical Instruments, Inc., Fremont, CA) and streptavidin (SADH) biosensors from FortéBio (Part #19-0130). Experiments utilized a consistent running buffer composed of HBS-T (HEPES-buffered saline, 10 mM HEPES, 150 mM NaCl, pH 7.4 with 0.005% Tween-20). To prevent buffer mismatch response upon sample injection, all samples were diluted from a concentrated deionized water stock into this running buffer such that the difference in buffer composition was negligible. Buffers were filtered using 0.45 μm pore filters prior to use.

All experiments began with priming the system with running buffer three times, followed by installation of the streptavidin (SADH) sensor chip. All three flow cells were checked for alignment of the SPR angle. The sensor was conditioned using 50 mM NaOH in deionized water over all flow cells at 50 μL/min for 1 min. The biotinylated 12-mer sense strands were immobilized to the surface of the flow cell 1 (FC1) by manual injection of 100 nM solution at 10 μL/min until a capture response of approximately 60−70 RU was seen. FC2 was used as a reference cell with no target immobilized. To block any potential unreacted streptavidin sites, 20 μM biotin (Aldrich, CAS #58-85-5) in running buffer was flowed over all cells (FC1, FC2, and FC3). Buffer solution was injected over all flow cells at 50 μL/min for 30 s twice prior to running any assay to ensure that responses were consistent and that the signal returned to baseline following injections.

Dilution series of all analytes to be tested were made such that two-fold, five-point concentration ranges were made in running buffer unless otherwise specified. The appropriate concentration range for each analyte was determined via initial manual injection experiments (data not shown). Experiments were run in succession on the same flow cell at 50 μL/min, with 180 s for analyte injection and approximately 300−600 s for dissociation (unless otherwise noted). Each injection cycle was followed by injection of 10 mM HCl for 30 or 60 s to regenerate the surface as was determined from trials of manual injections to re-establish the original baseline. Each experiment conducted was performed at least in duplicate, and reported analytical data represent an average of these experimental results.

All data were obtained using Pioneer Instrument Software version 4.3.1, build 32. Analysis of sensograms to obtain the RU binding amplitude, on rates, off rates, and affinity measurements was performed using Qdat Data Analysis Tool, version 4.3.1 build 2. All curves were fit to a bimolecular reaction using the global nonlinear least squares regression Analysis Tool, first for only the off rate, then the off rate was fixed once to help solve for the on rate before finally global fitting on rates, off rates and RUmax.

UV Thermal Melt T_m Measurement of OPNAs. The 10mer OPNA oligomers in Table 1 were evaluated for their binding affinity for the complementary 10mer DNA by measuring T_m values as described below. A mixed solution of 4 μM 10mer OPNA oligomer and 4 μM complementary 10mer DNA in 4 mL aqueous buffer (pH 7.16, 10 mM sodium phosphate, 100 mM NaCl) in a 15 mL polypropylene falcon tube was incubated at 90 °C for a minute and slowly cooled to ambient temperature. Then, the solution was transferred into a 4 mL quartz UV cuvette and the absorbance measured at 260 nm on a UV/visible spectrophotometer (Agilent 8453 UV/visible) while increasing the temperature by 0.5 or 1 °C/min. The sense single strand 10mer DNA for T_m measurement were purchased from Bioneer (www.bioneer.com, Dajeon, Republic of Korea) and used without further purification. The observed T_m values (uncorrected) for the OPNA derivatives hybridized

Table 2. Nucleotide Sequences of the Complementary Antisense Strand and Biotin-Immobilized ssDNA Sense Strand[a]

Code	Oligonucleotide Description	Nucleotide Sequence
AS-OPNA 10mer	Antisense Strand with OPNA Modifications	5'- GT**AGATCACT** - 3'
Sens-b-ssDNA-2Mut	Sense 5'-Biotin-ssDNA 12mer 2Mut (8 bpc)	3'- *G*-<u>AT</u>TCTAGTGA-*C*- 5'
Sens-b-ssDNA-1Mut	Sense 5'-Biotin-ssDNA 12mer 1Mut (9 bpc)	3'- *G*-<u>A</u>ATCTAGTGA-*C*- 5'
Sens-b-ssDNA-WT	Sense 5'-Biotin-ssDNA 12mer WT (10 bpc)	3'- *G*-CATCTAGTGA-*C*- 5'

[a]Bold: OPNA antisense strand with all modification sites; underline: mutation sites on the immobilized biotin sense strand; italic: added spacer nucleotides, no complementary OPNA base.

to the 10mer ssDNA are provided in Table 1. Experiments performed with 1 and 2 mutations in the Sense ssDNA and selected OPNA designed to evaluate the specificity of binding are described in the Supplementary Information section. A thermal UV melt assay designed to evaluate the T_m dependence with increasing sodium chloride is presented in the Supplementary Information section. T_m measurements were performed using GraphPad Prism and a two-state unfolding model fitting for T_m and native, unfolded baselines. Additional information is in the Supplementary Information section.

RESULTS AND DISCUSSION

OPNA Chemistry. Peptide nucleic acids (PNA) are a novel class of artificial nucleic acids developed by Nielsen et al., in 1991.[6] Despite its attractive properties resembling natural DNA or RNA, PNA oligomers have never been developed as therapeutic agents due to poor cell permeability and physicochemical properties. To overcome these limitations, there have been several different approaches to modify PNA such as covalent incorporation of cell penetrating peptides and incorporating PNA monomer(s) with a backbone of positively charged 2-aminoethyl-lysine or 2-aminoethyl-arginine in place of 2-aminoethyl glycine.[11,18,39] OliPass PNA (OPNA) is a chemically modified PNA which is composed of original/unmodified monomers and modified monomers possessing nucleobases covalently linked with a positively charged group such as an amino-alkyl moiety (Figure 1). One of the advantages of adding the amino-alkyl moiety to the nucleobase, rather than the PNA backbone, is that the resultant compounds remain achiral. In addition, since there are no stereoisomers, the OPNA monomers easily increase structural diversity. Importantly, the cationic/amino-alkyl character of the OPNA may allow it to be passively embedded into the cell membrane through electrostatic interactions with anion moieties on the surface of cell membranes. Once embedded in the cell membrane, an OPNA may localize inside via presumably passive diffusion or endocytosis. Table 1 shows the OPNA oligomers used in this study.

Confirmation of heterodimerization between the OPNA ASO and the corresponding ssDNA sense strand was performed first by thermal shift assays and then by surface plasmon resonance (SPR) kinetics. The T_m values for the OPNA-ssDNA studies using the WT Sense ssDNA 10mer strand (3'-CATCTAGTGA-5', Table S1) are shown in Table 1. The thermal stability increases with increasing amino-alkyl-base modification (51 to 69 °C). Experiments were also performed with 1 and 2 mutations in the Sense ssDNA and selected OPNA to evaluate the specificity of binding (Table S1). Table S2 in the Supporting Information section shows that both OPNA-1A and OPNA-1C have a decrease of −9.6 and −8.1 °C, respectively, binding to a ssDNA sense strand with 1 internal mutation and a larger decrease of −17.9 and

−15.6 °C binding to the sense strand with two internal mutations. The triple cation modification OPNA-2A1C decreases −19.2 °C binding to the 1 internal mutation sense strand. These studies suggest that despite the amino-alkyl substitutions and apparent high affinity, the OPNA are sensitive to mismatch sequences which should contribute to specificity of binding.

Hybridization Kinetics of the Cationic/Amino-Alkyl-Base-Modified PNA Antisense Strand to ssDNA Sense Strand. A series of SPR kinetic studies were performed to evaluate the kinetics and thermodynamics of hybridization of seven AS OPNA oligonucleotides (Table 1) to immobilized biotinylated sense strand ssDNA to determine if the base-substituted amino-alkyl modifications have unfavorable or favorable effects on the kinetics.[20] The binding of AS OPNA to the complementary sense strand was achieved by flowing the OPNA over an immobilized 5′-biotin-labeled ssDNA sense strand bound to a streptavidin sensor. Table 2 shows the different 5′-biotin sense strands used in the experiments. Each of the 5′-biotin sense strands was designed to have the OPNA 10mer bases bind to a 12mer DNA sequence where a single nonsense base was added to the 3′ and 5′ ends leading to hybridization only to the central complementary 10 bases. Initial kinetic studies were performed measuring the kinetics of the 10mer ssDNA-Cntrl control to the sense sequence Sense-b-ssDNA-WT that contained all 10 of the complementary nucleotide bases. Binding of the ssDNA-Cntrl AS (sequence 5′→3′ GTAGATCACT) to the immobilized wild-type sense strand resulted in an association rate, k_a, and dissociation rate, k_d, of 6.5×10^4 M^{-1} s^{-1} and 4.6×10^{-3} s^{-1}, respectively, at 20 °C. The hybridization equilibrium dissociation constant (K_d) was calculated from the ratio k_d/k_a and has a moderate binding affinity of $K_d = 72$ nM (20 °C, data not shown). Kinetic studies with the PNA control (OPNA-0) binding to the wild type DNA biotin-sense strand (Sense-b-ssDNA-WT, containing the full 10 nucleotides that can complement with OPNA), bound, however, with a very high affinity ($K_d < 5$ nM) at 30 °C and essentially irreversibly at 20 °C with a $k_d < 1 \times 10^{-5}$ s^{-1} (half-life $t_{1/2} > 19$ h). Because the curves associated with binding did not reflect reversible two-state binding, neither the binding rates nor the binding constant could be determined accurately for the OPNA ASO (data not shown).

Binding studies were then performed using one or two 3′ mutations on the 3′ end of the Sense-b-ssDNA-WT complementary sequence (Table 2). Preliminary studies showed that very good association and dissociation binding curves could be generated at both 20 and 30 °C using two terminal mutations on the 3′ end of the immobilized sense strand, referred to as Sense-b-ssDNA-2Mut. Table 2 shows that the two 3′ mutations replace the terminal wild type sequences 3′-CA with 3′-AT which prevents base pairing with the 5′ OPNA sequence of 5′-GT. It should also be noted that these two mutations do not prevent hybridization to any of the

Table 3. OPNA SPR Binding Kinetics to Sens-b-ssDNA-2Mut (Hybridization to 8 Complementary Base Pairs)

Analyte	20 °C			25 °C			30 °C		
	k_a x10^5 (M^{-1}s^{-1})	k_d x10^{-3} (s^{-1})	K_d (nM)	k_a x10^5 (M^{-1}s^{-1})	k_d x10^{-3} (s^{-1})	K_d (nM)	k_a x10^5 (M^{-1}s^{-1})	k_d x10^{-3} (s^{-1})	K_d (nM)
OPNA-0	0.4 ± 0.04	1.7 ± 0.1	43.0 ± 2.3	0.84 ± 0.04	7.8 ± 0.6	93.0 ± 12	2.1 ± 0.6	30. ± 1.0	140 ± 11
OPNA-1A	3.1 ± 1.1	0.37 ± 0.2	1.2 ± 0.4	7.3 ± 0.71	2.4 ± 0.1	3.3 ± 0.2	8.0 ± 1.9	8.6 ± 0.5	11 ± 2
OPNA-1G	2.9 ± 0.8	1.1 ± 0.1	3.8 ± 0.7	6.3 ± 0.6	5.0 ± 0.3	7.9 ± 0.2	5.9 ± 1.3	19. ± 1.0	35 ± 7
OPNA-1C	2.3 ± 0.9	0.32 ± 0.05	1.4 ± 0.7	6.2 ± 2.9	2.1 ± 0.4	3.4 ± 1.1	7.2 ± 3.0	6.4 ± 1.6	9 ± 2
OPNA-2A								3.2 ± 2.2	
OPNA-3A								0.27 ± 0.13	
OPNA-2A1C								0.22 ± 0.17	

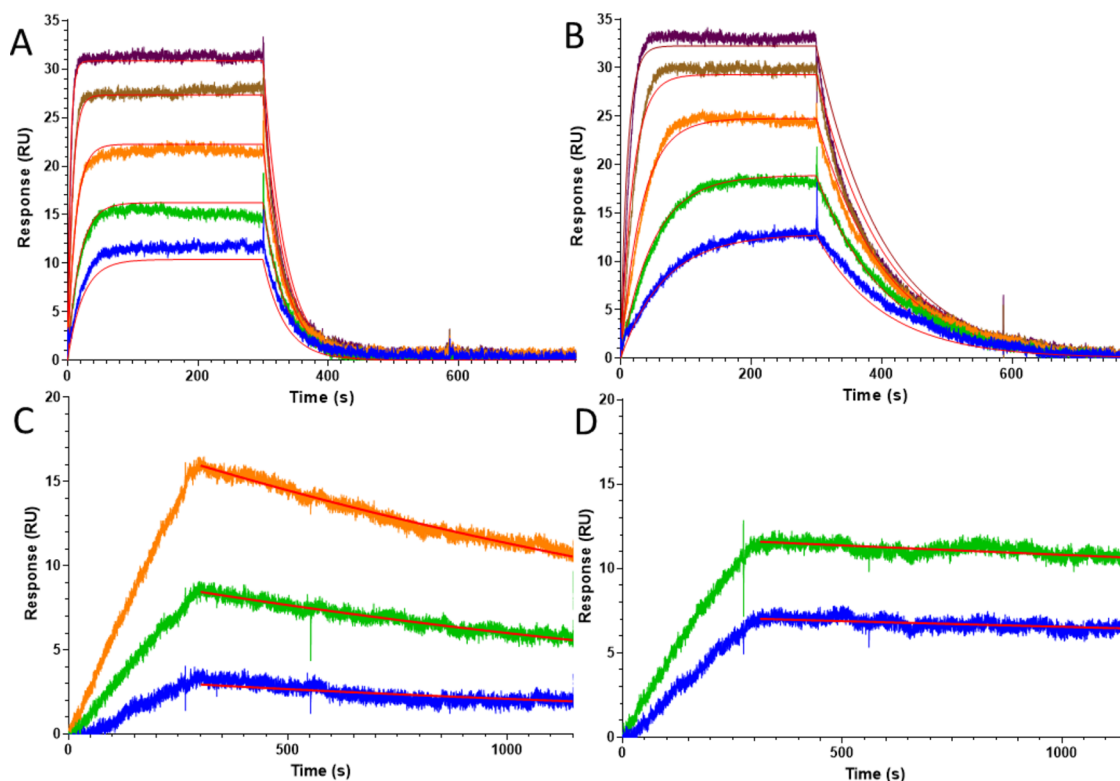| Analyte	20 °C			15 °C			10 °C		
	k_a x10^5 (M^{-1}s^{-1})	k_d x10^{-3} (s^{-1})	K_d (nM)	k_a x10^5 (M^{-1}s^{-1})	k_d x10^{-3} (s^{-1})	K_d (nM)	k_a x10^5 (M^{-1}s^{-1})	k_d x10^{-3} (s^{-1})	K_d (nM)
ssDNA-Cntrl	1.7 ± 0.1	450 ± 51	2,600 ± 450	1.5 ± 0.06	130 ± 18	870 ± 80	1.25 ± 0.2	37 ± 6	296 ± 7

Figure 2. OPNA SPR hybridization kinetics to Sens-b-ssDNA-2Mut. (A) OPNA-0 control PNA titration; (B) OPNA-1A titration; (C) OPNA-2A titration; (D) OPNA-2A1C titration. Titration concentrations for OPNA-0 were 2-fold dilutions of 62.5 to 1000 nM (bottom to top curve). Titration concentration for OPNA-1A was 6.25 to 100 nM (bottom to top curve). Concentrations for OPNA-2A were 1.5, 3, 6 nM and for OPNA-2A1C were 1.5, 3 nM. Titrations performed at 30 °C. The red line is the global nonlinear least squares fit; values in Table 3.

OPNA nucleotides that have amino-alkyl-base modifications, and it is expected that the kinetic results using the OPNA-modified strands should not be greatly influenced by the adjacent two 3′-sense strand mutations. The binding affinity of the 10mer ssDNA-Cntrl control to the Sense-b-ssDNA-2Mut, which can hybridize to only 8 base pairs, was much weaker than that observed for the wild type Sens-b-ssDNA-WT containing a 10 base pairs consensus sense stand. Table 3 shows that the K_d for ssDNA-Cntrl binding to Sense-b-ssDNA-2Mut was 2.6 μM and the rate constants k_a and k_d were 1.7 × 10^5 M^{-1} s^{-1} and 0.45 s^{-1}, respectively, at 20 °C. The primary effect on the kinetics when hybridizing to 2 fewer nucleotides is an ~100-fold increase in the rate of dissociation. The k_a rate is very similar (~1 × 10^5 M^{-1} s^{-1}) to that reported by others measuring 9 to 16mer DNA/DNA hybridization and demonstrates that association rates are not strongly dependent on the length of nucleotide base pair types.[29,40−43] The values of dissociation rates, however, are very dependent on the

length and nucleotide sequence and have been reported to vary 100−1000-fold for short 10−14mer ASO.[29,40]

The first set of experiments for the OPNA oligonucleotides binding to Sense-b-ssDNA-2Mut was with the unmodified PNA (OPNA-0) to compare to both the ssDNA-10mer control and modified OPNA-1A, OPNA-1G, and OPNA-1C oligomers. Figure 2A shows that the SPR kinetic binding curves for OPNA-0 has a good concentration-dependence leading to a maximum response consistent with near saturation of the immobilized Sense-b-ssDNA-2Mut (8 bp consensus) target. One of the key experimental designs for these SPR studies was to minimize the loading of the Sense-b-ssDNA-2Mut strand to prevent a commonly observed mass transport diffusion artifact that inhibits an accurate analysis of rate constants.[44,45] In these studies, the total load of Sense-b-ssDNA-2Mut onto the sensor chip was kept at a minimum where the mass loaded to the sensor provided only ~60 RU. This low load would then minimize the mass transport issue
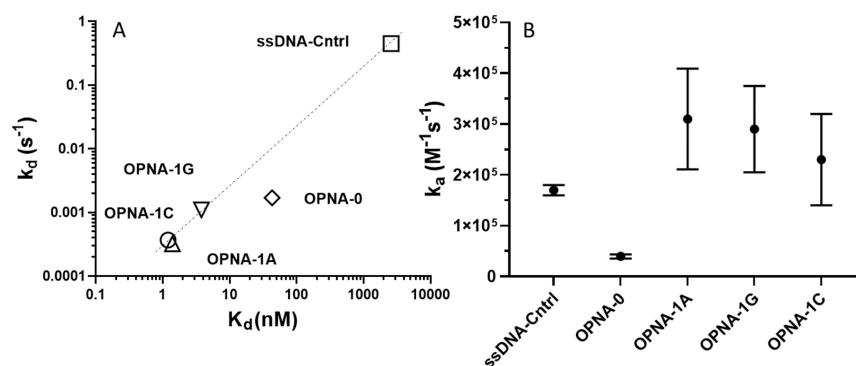
Figure 3. Comparison of hybridization rate constants and affinity for ssDNA-Cntrl control, unmodified OPNA-0, and modified OPNA-1A, OPNA-1G, OPNA-1C at 20 °C. (A) k_d dissociation rates vs K_d affinity values (the dashed line is a visual aid, not a fitted line); (B) k_a association rates.

and would produce a maximum signal upon full binding of the ASO strands to the Sense-b-ssDNA-2Mut of only ∼30 RU which is exactly what is observed in Figure 2. Literature search of previous SPR studies find that many of the early studies did not use low immobilized target densities (eg., RU Loads ∼3000 and RUmax ∼2000) which may have affected the final kinetic analysis and led to underestimating/overestimating values.[46] Confirmation that the bimolecular binding is a two-state event and not influenced by mass transport diffusion is supported by the very good bimolecular nonlinear least square fit (solid red line in Figure 2A).

A global fit of the five curves indicated the binding affinity of OPNA-0 to Sense-b-ssDNA-2Mut increased ∼60-fold (K_d decrease to 43 nM) compared to the ssDNA-Cntrl control. This increase in affinity was driven by a 260-fold decrease in the k_d dissociation rate and an ∼4-fold decrease in the k_a association rate, as seen in Figure 3 (20 °C). The increase in affinity for OPNA-0 compared to ssDNA-Cntrl is consistent with previous observations and predicted to be due to the lack of a negatively charged phosphate backbone for the PNA in the OPNA-ssDNA complex as compared to the two-phosphate backbone ion-ion repulsions that occurs for dsDNA complexes.[41,47−49]

SPR binding studies were performed to evaluate the effect that nucleotide base amino-alkyl modifications had on the binding affinity and hybridization kinetics to ssDNA. Three OPNA strands containing only a single amino-alkyl modification on either adenine, guanine, or cytosine bases (Table 1) were studied. The SPR hybridization binding curves of OPNA-0 vs OPNA-1A are shown in Figure 2. Visual comparison of the binding curves of OPNA-1A to the OPNA-0 nonmodified PNA (Figure 2) shows that there is a clear decrease in the dissociation rate of the modified OPNA-1A vs OPNA-0. Kinetic rates and binding affinity were obtained from the global fit of each data set, and the results for all 3 modified OPNA are shown in Figure 3 and Table 3. The data in Table 3 indicate that the modified OPNA have a significant 10−30-fold lower K_d vs the OPNA-0 control (20 °C). The higher thermal melting T_m for the modified OPNA also correlate with higher affinity vs the OPNA-0 control (Table 1). Figure 3A shows that the dissociation rate for the OPNA-modified AS strands had an even more favorable ∼2−5 fold slower k_d than OPNA-0 (e.g., OPNA-1A 0.3×10^{-3} s^{-1} vs OPNA-0 1.7×10^{-3} s^{-1} at 20 °C). Figure 3A also shows that the primary driver for the favorable K_d decrease from ssDNA-Cntrl to the modified OPNA strands is due to an ∼1000-fold decrease in the dissociation rate as seen by the approximately

linear correlation. In addition, the association rate, k_a, for the OPNA-modified strands increased 5−7-fold compared to OPNA-0 (Figure 3B), suggesting that the addition of the cationic/amino-alkyl modification helped promote binding. The magnitude of the observed k_a rates is consistent with that observed by a wide range of kinetic studies performed with short nucleotides.[29,40,41,43,47] Together, the decrease in k_d and increase in k_a for the OPNA-modified strands led to an ∼10−30 fold increase in affinity compared to the OPNA-0 PNA control, Figure 3A.

While previous OPNA studies have demonstrated that amino-alkyl modifications promote cell-based activity (unpublished data) prior to this kinetic study, there was no quantitative information on how the cation OPNA modifications of the bases might affect the affinity (K_d) of base pairing and or double strand complex formation.[21−24] These current SPR kinetic studies suggest that hybridization with the amino-alkyl modifications further promoted hybridization due to more favorable dissociation and association rates. The fact that the dissociation rate is slower for the modifications compared to OPNA-0 suggests the alkyl extension or cationic/amino group or both promotes interactions with the adjacent ssDNA strand to stabilize the complex. Similarly, the increase in the association rate for OPNA-modified strands suggest that the cationic/amino-alkyl promotes a new interaction that favors binding. This increase in affinity for the OPNA-modified strands provides an additional rationale for introducing the unique OPNA amino-alkyl group to the PNA oligomers in addition to promoting favorable cell permeability. This has proven to be a powerful combination and it has allowed the OPNA-based molecule OLP-1002 to be advanced into phase one and phase two human clinical trials.[26−28]

Hybridization Thermodynamic Analysis. Performing temperature-dependent kinetic binding studies provides insight into the thermal stability of hybridization and identifies effects on the association and dissociation rate constants which can provide information on molecular interactions that drive the dimerization event. SPR studies were performed at 20, 25, and 30 °C for OPNA-0, OPNA-1A, OPNA-1G, and OPNA-1C and at 10, 15, and 20 °C for ssDNA-Cntrl, and the results are shown in Table 3. Inspection of the k_a values for each of the ASO with respect to temperature shows that the k_a rate for each ASO is marginally sensitive to an increase in 10 °C (e.g., OPNA-1A 3.1×10^5 M^{-1} s^{-1} at 20 °C vs 8.0×10^5 M^{-1} s^{-1} at 30 °C). This relative insensitivity for the on rate is a common observation reflecting that elevated solvent energetics is not strongly dependent on diffusion and bimolecular recognition/

initiation at these moderate temperatures.[50] However, the dissociation rate k_d for each ASO increases exponentially with temperature and is ~10- to 20-fold faster for each ASO at 30 °C versus 20 °C (e.g., OPNA-1A 0.37×10^{-3} s^{-1} at 20 °C vs 8.6×10^{-3} s^{-1} at 30 °C). The thermally sensitive molecular interactions that lead to increased dissociation rates are due primarily to the weakening of base pair hydrogen bonds, dipole stacking interactions, and increased fraying of the 5′ and 3′ ends. The thermal effects on k_a and k_d are consistent with other DNA−DNA and PNA-DNA hybridization systems.[40,41]

The equilibrium dissociation constants (K_d) calculated from the SPR hybridization rate constants for experiments performed at different temperatures are presented in Table 3 for each of the OPNA. As seen for OPNA-1A the affinity decrease with increasing temperature from 20 to 30 °C (1.2 to 11 nM, respectively) is consistent primarily with the fold increase in the dissociation rate, k_d. The average fold change in K_d for all 4 OPNA from 20 to 30 °C is ~3 to 10-fold. While these temperature-dependent changes in kinetic rates and affinity can provide insight into the molecular interactions mediating the hybridization (e.g., 3-D diffusion, base pair formation/initiation and hybridization zippering, and confirmation of 2-state bimolecular binding),[50] information regarding the energetic contributions toward hybridization can be provided by calculating the free energy of binding, ΔG, as well as the enthalpy, ΔH, and entropy of binding, ΔS, with the relationship $\Delta G = \Delta H - T\Delta S$ describing the full thermodynamic relationship. The free energy is also a function of the equilibrium association binding constant (K_a), $\Delta G = -RT\ln(K_a)$, where the association binding constant K_a can be calculated from the kinetic derived affinity $1/K_d$, R is the universal gas constant, and T is the temperature in Kelvin.

A full thermodynamic characterization of the hybridization reactions can be determined using the van't Hoff Plot that linearizes the relationship of K_a to inverse temperature giving $\ln(K_a) = -\Delta H/RT + \Delta S/R$ which enables the determination of both the enthalpy and entropy of binding from the temperature-dependent SPR kinetic experiments. Figure 4
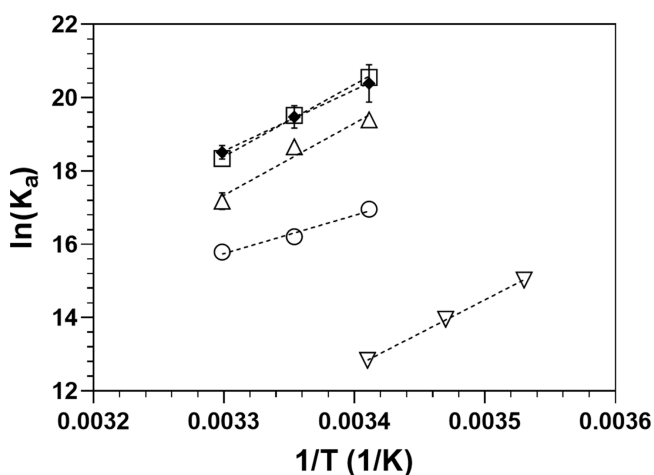
shows the van't Hoff plot and graphically indicates a linear relationship between $\ln(K_a)$ and the inverse temperature which, because the response is linear, permits calculations of the enthalpy, ΔH, and entropy, ΔS, of hybridization when the ΔC_p is approximately zero. Table 4 shows the van't Hoff Plot-derived ΔH, ΔS, and corresponding calculated ΔG for each of the OPNA ASO and ssDNA-Cntrl at three temperatures. The entropy contribution to the free energy, $-T\Delta S$, for OPNA-0, OPNA-1A, OPNA-1G, and OPNA-1C shown in Table 4 are +45, +114, +116, and +62.9 kJ/mol, respectively, at 20 °C. These entropy terms are unfavorable energetically and likely due primarily to the induced conformational constraint of the unstructured flexible single strand upon formation of the constrained double-strand helical structure as well as solvent effects. Similar unfavorable entropy values are seen for classical dsDNA complexes as seen for the ssDNA-Cntrl in Table 4 and has also been observed for other thermodynamic studies for both DNA−DNA and PNA-DNA hybridization.[40,41,51−53] It is interesting that the $-T\Delta S$ entropy values for the OPNA modified ASO are less favorable than OPNA-0 which may suggest that there is an additional unfavorable loss of degrees of freedom for the amino-alkyl polymer upon forming an OPNA-DNA double strand complex.

A comparison of the entropy and enthalpy values in Table 4 clearly indicates that enthalpy of binding, ΔH, promotes overall double strand hybridization for all of the ASO studied. The DNA−DNA hybridization ΔH for the AS control ssDNA-Cntrl (8 bases pairs complementing to the Sense-b-ssDNA-2Mut) has a value of −151 kJ/mol which compares well to the nearest-neighbor thermodynamic prediction model by Santa-Lucia et al. with a predicted ΔH of −214 kJ/mol for the same 8mer sequence.[54,55] A thermodynamic 10mer study by Schwarz et al., observed hybridization ΔH values for different DNA−DNA sequences of −120 to −220 kJ/mol. In the same study, they measured the enthalpy of binding for the same sequences of PNA-DNA complexes and found ΔH values of −90 to −128 kJ/mo.[49,53] No clear explanation has been identified for these PNA lower ΔH values.

Figure 5 shows that the ΔH values for the amino-alkyl modified OPNA are significantly larger than the OPNA-0 PNA control. The ΔH for OPNA-1A and OPNA-1G (−165 and −164 kJ/mol, respectively) are twofold larger than OPNA-0 (−86 kJ/mol), suggesting that the similar amino-alkyl modification in OPNA-1A and OPNA-1G (Table 1: A(5), G(5)) provides unique favorable interactions for the overall hybridization event. When normalized by the number of base pairs per heterodimer (8 for the Sense-b-ssDNA-2Mut sense strand), the enthalpy of binding per base pair of OPNA-0, OPNA-1A, OPNA-1G, and OPNA-1C is −10.7, −20.6, −20.5, and −14 kJ/mol, respectively. These favorable enthalpies per base pair values represent the stabilizing energetics that originate from the 2 or 3 Watson-Crick Hydrogen bonds for A:T and G:C pairs, respectively, base pair / base pair dipole stacking energetics, as well as an unknown stabilizing interaction from the alkyl-cation modification. Finally, the observation that the OPNA cationic/amino-alkyl modifications provide an increase of approximately −80 kJ/mol for the ΔH per OPNA-DNA complex along with favorable kinetics involving slow dimer dissociation provides evidence, for the first time, that the addition of cationic/amino-alkyl-base modifications to PNA ASO provides not only an advantage toward improved cell permeability through the introduction of cations on nucleotide bases but also a thermodynamic

Figure 4. Van't Hoff plot to calculate enthalpy and entropy values from the ASO hybridization kinetic studies. Circle: OPNA-0; Square: OPNA-1A; Up Triangle: OPNA-1G; Diamond: OPNA-1C; Down Triangle: ssDNA-10mer. Equilibrium association constant (K_a) derived from the K_d value shown in Table 3. Enthalpy and entropy values for each ASO derived from the linear plots are reported in Table 4.

Table 4. Kinetic-Derived Thermodynamic Characterization of Hybridization (8 Base Pair Hybridization)

Analyte	ΔH (kJ/mol)[a]	ΔS (J/molK)[a]	20° C			25° C			30° C		
			-TΔS (kJ/mol)	ΔG (kJ/mol)[c]	K_d (nM)[c]	-TΔS (kJ/mol)	ΔG (kJ/mol)[c]	K_d (nM)[c]	-TΔS (kJ/mol)	ΔG (kJ/mol)[c]	K_d (nM)[c]
OPNA-0	-86 ± 4	-155 ± 14	45.6	-41.2	46.0	46.4	-40.4	83.6	47.1	-39.6	149.0
OPNA-1A	-165 ± 11	-390 ± 37	114.3	-50.2	1.1	116.3	-48.3	3.5	118.2	-46.3	10.4
OPNA-1G	-164 ± 20	-396 ± 66	116.0	-47.7	3.1	118.0	-45.7	9.7	120.0	-43.8	28.8
OPNA-1C	-112 ±22	-215 ± 73	62.9	-49.1	1.8	64.0	-48.0	3.9	65.0	-46.9	8.2
ssDNA-Cntrl	-151 ± 7	-408 ± 23	120	-31.4	2,545	122	-29.4	7,194	124	-27.3	19,648
Nearest Neighbor Predicted ΔH and ΔS for ssDNA 8mer binding sequence[b]											
ssDNA 8mer[b]	-214	-619.0	181	-32.9	1,350	185	-29.8	4,807	188	-26.8	17,115

[a]Experimental thermodynamic values calculated using the ΔH and ΔS from the van't Hoff Plot; binding to sense-b-ssDNA-2Mut for an 8mer complementary sequence. [b]Theoretical prediction using the nearest neighbor model for only 8 complementary nucleotides (sequence that binds to the Sens-b-ssDNA-2Mut). [c]ΔG and K_d values calculated from ΔH and ΔS values (K_d values are not from Table 3).
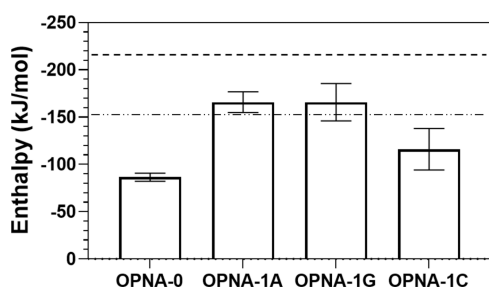

Figure 5. Van't Hoff-derived enthalpy of ASO hybridization to the Sense-b-2Mut ssDNA. The OPNA-0, OPNA-1A, OPNA-1G, and OPNA-1C data were derived from Table 4. The lower dash-dot line represents the ΔH for the ssDNA-Cntrl control (−151 kJ/mol). The dark dashed line at the top is the predicted Nearest Neighbor ΔH (−214 kJ/mol) for an 8mer ssDNA binding to the 2Mut -ssDNA sense strand.

advantage increasing overall hybridization affinity compared to PNA ASO. While no specific molecular mechanism has been identified that explains the approximate −80 kJ/mol increase in favorable ΔH with an amino-alkyl modification, its magnitude is consistent with that expected for a favorable ion-ion electrostatic interaction between the OPNA cationic/amino-alkyl group and a phosphate from the paired ssDNA perhaps, suggesting that the base cation can extend to the DNA phosphate backbone or form a salt bridge.[56] Thermal UV melt experiments were performed with OPNA-1A and OPNA-1C to determine if association is salt-dependent. Table S3 shows that OPNA-1A and OPNA-1C have a decrease in T_m thermal stability, −4.9 and −8.1 °C, respectively, when the buffer has 100 mM sodium chloride vs 900 mM sodium chloride in 10 mM sodium phosphate, pH 7.0. The noncation OPNA-0 T_m decreased −2.6 °C. This result suggests that the cation may interact in an ionic electrostatic interaction with the phosphate backbone of the ssDNA sense strand.

Estimates of the affinity for oligonucleotide hybridization at 37 °C can provide important information on the values of dissociation rate constants, k_d, and dissociation half-life ($t_{1/2}$) which are factors determining the residence time that the ASO is bound to the intracellular target sense strand at physiological temperatures. Using the ΔH and ΔS for each OPNA the K_d calculation at 37 °C for OPNA-0, OPNA-1A, OPNA-1G, OPNA-1C binding to the 8 base pair sense strands are 323, 38, 116, and 23 nM, respectively. Using these K_d values and assuming a k_a value of 7×10^5 M^{-1} s^{-1} (average for the k_a values at 30 °C), the k_d dissociation rate values increase significantly from 30 to 37 °C for OPNA-0 from 30×10^{-3} to

220×10^{-3} s^{-1} ($t_{1/2}$ 3 s), OPNA-1A from 8.6×10^{-3} to 26×10^{-3} s^{-1} ($t_{1/2}$ 26 s), OPNA-1G from 19×10^{-3} to 81×10^{-3} s^{-1} ($t_{1/2}$ 8 s), and OPNA-1C from 6.4×10^{-3} to 16×10^{-3} s^{-1} ($t_{1/2}$ 42 s). These high rates of dissociation may not be desirable for an ASO drug at physiological temperature, and this is an example of how DNA ASO kinetic and thermodynamic studies, as presented here, can provide guidance on optimizing both kinetic and affinity properties in a preclinical setting as well as justify developing PNA-like antisense drugs. One strategy to achieve higher affinity is to use longer oligomers. Another strategy to achieve improved affinity is to incorporate more than one amino-alkyl-base modification per PNA strand which is described below.

Kinetics of Multiple OPNA Cationic/Amino-Alkyl-Base Modifications. The addition of a single cationic/amino-alkyl modification demonstrates multiple advantages in enhancing AS hybridization including increasing the affinity, a proportional decrease in the dissociation rate, promoting favorable enthalpy of binding (ΔH), and improved cell permeability. Studies were performed to also explore the effect multiple modifications would have on AS hybridization. Table 1 lists 3 additional OPNA modifications including incorporating 2 Adenine modifications in one strand (OPNA-2A), 3 Adenine modifications in one strand (OPNA-3A), and 2 Adenine and 1 Cytosine modification in one strand (OPNA-2A1C). Figure 2C,D shows that the hybridization SPR curves of OPNA-2A and OPNA-2A1C at 30 °C are very different compared to OPNA-0 and OPNA-1A. OPNA-2A and OPNA2A1C have association phases that are nearly linear and have dissociation phases that are very slow and look "irreversible". Experimental concentrations were varied to try and enhance binding curvature, but none were successful. The nature of these curves is typical for a tight binding interaction with a slow off rate and rather than fit both the association rate and dissociation rate the curves were fit for only the "apparent" k_d to the dissociation curve. The k_d fit to the data is shown in Figure 2C,D, and the values for these two OPNA and the OPNA-3A are shown in Table 3 at 30 °C. Binding studies were unsuccessful at 20 and 25 °C because the dissociation was even slower (essentially flat) and unable to fit an accurate k_d value. The k_d rates from Table 3 are plotted in Figure 6 and demonstrate that there is an approximate logarithmic decrease in the k_d with an ~100-fold change from 0 modifications (OPNA-0, k_d 30×10^{-3} s^{-1}) to 3 modifications (OPNA-3A, k_d 0.27×10^{-3} s^{-1}), resulting in an ~3−10-fold decrease in the dissociation rate per amino-alkyl modification added at 30 °C. In this figure, both OPNA with 3 modifications (OPNA-3A
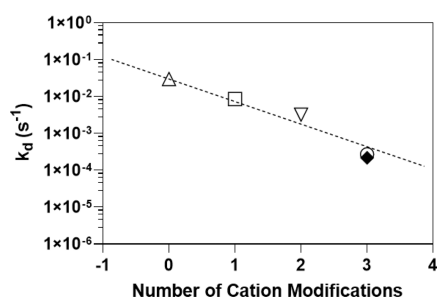
Figure 6. Dependence of the dissociation rate on the number of OPNA alky-cation modifications. Triangle-up: OPNA-0; Square: OPNA-1A; Triangle-down: OPNA-2A; Circle: OPNA-3A; Diamond: OPNA-2A1C.

and OPNA-2A1C) have a similar k_d, even though one has three adenine modifications and the other 2 adenine and 1 cytosine modification which suggest that the 1A(5) and 1C(102) chemical type of modifications has similar kinetic properties (also similar for OPNA-1A and OPNA-1C). The slower dissociation rate for the amino-alkyl modifications compared to OPNA-0 suggests the alky or cation or both promotes favorable interaction with the adjacent ssDNA strand to stabilize the complex including possible ionic-ionic interactions with the cationic/amino-alkyl and phosphate backbone of ssDNA or salt bridge. Based on the decrease in k_d trends above, it is likely that the addition of 3 modifications will also favorably increase the affinity >30-fold compared to the OPNA-1A modification. Assuming a 3 modification OPNA has a k_d value of ~0.3×10^{-3} s^{-1} ($t_{1/2}$ 2300 s, 38 min) at 30 °C and a $k_a \sim 10^5$ M^{-1} s^{-1}, the predicted K_d values would be approximately 0.3 nM. These results suggest that the unique cationic/amino-alkyl design of OPNA along with the addition of multiple modifications and longer oligonucleotide lengths might result in very potent picomolar affinity ASO at physiological temperatures, thus enhancing their role in antisense therapy applications.

CONCLUSIONS

Antisense technology has begun to show value in treating a wide range of diseases. One of the limitations toward using PNA antisense oligomers more widely is the fact that the PNA oligomers have low cellular permeability and require high concentrations as well as vehicle formulations to improve permeability. OPNA AS contain amino-alkyl-modified nucleotide bases and have improved cellular permeability. In this study, we have performed a systematic kinetic and thermodynamic analysis of OPNA-DNA hybridization to determine what effect the cationic/amino-alkyl modifications might have toward the formation of a stable complex. The kinetic studies demonstrated that a single amino-alky modification can reduce the k_d by ~2−5 fold and along with increases in k_a can increase the affinity by 10−30 fold. Kinetic studies with OPNA containing up to 3 amino-alkyl modifications per strand reduced the k_d by ~100-fold compared to OPNA-0 PNA control and likely increases the overall apparent affinity of OPNA-DNA by a similar fold (consistent with elevated thermal shift T_m values). The results from the temperature-dependent kinetics indicate that there is a strong increase in favorable ΔH (additional −80 kJ/mol vs OPNA-0). This favorable interaction suggests that the cationic/amino-alkyl modification of the OPNA makes favorable interactions with the ssDNA strand. Together, these kinetic and thermodynamic

results provide additional reasons to develop these amino-alkyl-based modified OPNA as antisense oligos.

ASSOCIATED CONTENT

Supporting Information

The Supporting Information is available free of charge at https://pubs.acs.org/doi/10.1021/acsomega.3c03184.

> Thermal UV melt data; chemical synthesis of the individual amino-alkyl modified nucleic acid units; and oligo-OPNA synthesis as well as HPLC, NMR, and mass spectroscopy data (PDF)

AUTHOR INFORMATION

Corresponding Author

William T. Windsor − *Department of Chemistry and Chemical Biology, Stevens Institute of Technology, Hoboken, New Jersey 07030, United States;* ⓞ orcid.org/0000-0002-9903-1127; Email: wwindsor@stevens.edu

Authors

Frank Podlaski − *Department of Chemistry and Chemical Biology, Stevens Institute of Technology, Hoboken, New Jersey 07030, United States*

Stephen Cornwell − *Department of Chemistry and Chemical Biology, Stevens Institute of Technology, Hoboken, New Jersey 07030, United States*

Kenny Wong − *Department of Chemistry and Chemical Biology, Stevens Institute of Technology, Hoboken, New Jersey 07030, United States*

Brian McKittrick − *Department of Global Sciences & Strategy, OliPass Corporation, Yongin, Gyeonggi 17015, Republic of Korea*

Jae-Hun Kim − *Department of Monomer Research, OliPass Corporation, Suwon, Gyeonggi 16229, Republic of Korea*

Daram Jung − *Department of Oligo Sciences, OliPass Corporation, Yongin, Gyeonggi 17015, Republic of Korea*

Yeasel Jeon − *Department of Oligo Sciences, OliPass Corporation, Yongin, Gyeonggi 17015, Republic of Korea*

Kwang-Bok Jung − *Department of Monomer Manufacture, OliPass Corporation, Suwon, Gyeonggi 16229, Republic of Korea*

Peter Tolias − *Department of Biology, School of Natural and Behavioral Sciences, Brooklyn College, CUNY, Brooklyn, New York 11210, United States*

Complete contact information is available at:
https://pubs.acs.org/10.1021/acsomega.3c03184

Author Contributions

[#]F.P. and S.C. contributed equally to this work and are to be considered primary authors.

Notes

The authors declare no competing financial interest.

ACKNOWLEDGMENTS

(Department of QC/QA, OliPass Inc) for their technical support. We would also like to thank Dr. Peter Tolias (Director Chemistry and Chemical Biology department, Stevens Institute of Technology) for his support and helpful discussions.

◼ REFERENCES

(1) Scharner, J.; Aznarez, I. ASO Clinical Applications of Single-Stranded Oligonucleotides: Current Landscape of Approved and In-Development Therapeutics. *Mol. Ther.* **2021**, *29*, 540−554.

(2) Crooke, S. T.; Liang, X. H.; Baker, B. F.; Crooke, R. M. Antisense technology: A review. *J. Biol. Chem.* **2021**, *296*, No. 100416.

(3) Crooke, S. T. Molecular Mechanisms of Antisense Oligonucleotides. *Nucleic Acid Ther.* **2017**, *27*, 70−77.

(4) Gupta, A.; Mishra, A.; Puri, N. Peptide nucleic acids: Advanced tools for biomedical applications. *J. Biotechnol.* **2017**, *259*, 148−159.

(5) Montazersaheb, S.; Hejazi, M. S.; Charoudeh, H. N. Potential of peptide nucleic acids in future therapeutic applications. *Adv. Pharm. Bull.* **2018**, *8*, 551−563.

(6) Nielsen, P. E.; Egholm, M.; Berg, R. H.; Bushardt, O. Sequence-Selective Recognition of DNA by Strand Displacement with a Thymine-Substituted Polyamide. *Science* **1991**, *254*, 1497−1500.

(7) Nielsen, P. E. PNA Technology. *Mol. Biotechnol.* **2004**, *26*, 233−248.

(8) Siddiquee, S. A Review of Peptide Nucleic Acid. *Adv. Tech. Biol. Med.* **2015**, *03*, No. e100416.

(9) Sahu, B.; Chenna, V.; Lathrop, K. L.; Thomas, S. M.; Zon, G.; Livak, K. J.; Ly, D. H. Synthesis of conformationaly preorganized and cell-permeable guanidine-based γ-peptide nucleic acids (γGPNAs). *J. Org. Chem.* **2009**, *74*, 1509−1516.

(10) de Costa, N. T. S.; Heemstra, J. M. Evaluating the Effect of Ionic Strength on Duplex Stability for PNA Having Negatively or Positively Charged Side Chains. *PLoS One* **2013**, *8*, No. e58670.

(11) Zhou, P.; Wang, M.; Du, L.; Fisher, G. W.; Waggoner, A.; Ly, D. H. Novel binding and efficient cellular uptake of guanidine-based peptide nucleic acids (GPNA). *J. Am. Chem. Soc.* **2003**, *125*, 6878−6879.

(12) Nielsen, P. E. REVIEW Peptide Nucleic Acids (PNA) in Chemical Biology and Drug Discovery. *Chem. Biodivers.* **2010**, *7*, 786−804.

(13) Quijano, E.; Bahal, R.; Ricciardi, A.; Saltzman, W. M.; Glazer, P. M. Therapeutic Peptide Nucleic Acids: Principles, Limitations, and Opportunities. *Yale J. Biol. Med.* **2017**, *90*, 583−598.

(14) Singh, K. R.; Sridevi, P.; Singh, R. P. Potential applications of peptide nucleic acid in biomedical domain. *Eng. Rep.* **2020**, *2*, No. e12238.

(15) Zhao, X.-L.; Chen, B.-C.; Han, J.-C.; Wei, L.; Pan, X.-B. Delivery of cell-penetrating peptide-peptide nucleic acid conjugates by assembly on an oligonucleotide scaffold. *Sci. Rep.* **2015**, *5*, 17640.

(16) Gasparello, J.; Manicardi, A.; Casnati, A.; Corradini, R.; Gambari, R.; Finotti, A.; Sansone, F. Efficient cell penetration and delivery of peptide nucleic acids by an argininocalix[4]arene. *Sci. Rep.* **2019**, *9*, 3036.

(17) Cordier, C.; et al. Delivery of antisense peptide nucleic acids to cells by conjugation with small arginine-rich cell-penetrating peptide (R/W)9. *PLoS One* **2014**, *9*, No. e104999.

(18) Nielsen, P. E.; Haaima, G.; Lohse, A.; Buchardt, O. Peptide Nucleic Acids (PNAs) Containing Thymine Monomers Derived from Chiral Amino Acids: Hybridization and Solubility Properties of D-Lysine PNA. *Angew. Chem., Int. Ed.* **1996**, *35*, 1939−1942.

(19) Ortega, J. A.; Blas, J. R.; Orozco, M.; Grandas, A.; Pedroso, E.; Robles, J. Binding affinities of oligonucleotides and PNAs containing phenoxazine and G-clamp cytosine analogues are unusually sequence-dependent. *Org. Lett.* **2007**, *9*, 4503−4506.

(20) Chung, S.; Jung, D.; Cho, B.; Jang, K.; Yoon, H. Exon Skipping By Peptide Nucleic Acid Derivatives. W.O. Patent No. WO 2018/122610 Al, World Intellectual Property Organization 2018.

(21) Chung, S. et al. SCN9A Antisense Pain Killer. Patent CA3051178A1, Canadian Patent Application Preprint at 2018.

(22) Han, S.-Y.; Sung, K.; Hong, M.; Kang, D.; Heo, J.; Jang, K. Acetyl-Coa Carboxylase 2 Antisense Oligonucleotides. Patent WO 2020/036353 A1, World Intellectual Property Organization 2020.

(23) Chung, S.; Jung, D.; Cho, B.; Jang, K.; Yoon, H. HIF-1-Alpha Antisense Oligonucleotides. Patent WO 2018/069764 Al, World Intellectual Property Organization 2018.

(24) Chung, S.; Kim, H.-Y.; Park, H.-J.; Kim, M.-R.; Lee, J.-O. Peptide Nucleic Acid Derivatives with Good Cell Penetration and Strong Affinity for Nucleic Acid. US Patent 8,895,734 B2, U.S. Patent and Trademark Office 2014.

(25) Chung, S et al. SCN9 Antisense Pain Killer. US Patent 11,162,104 B2, U.S. Patent and Trademark Office 2021.

(26) OliPass Corporation. NCT05216341: Study of OLP-1002 Injections for Reducing Moderate to Severe Pain Due to Osteoarthritis in Hip and/or Knee Joint. https://clinicaltrials.gov/ct2/show/NCT05216341 2022.

(27) OliPass Corporation. NCT03760913: OLP-1002 is Being Studied in the Treatment of Pain. https://www.clinicaltrials.gov/ct2/show/NCT03760913 2020.

(28) OliPass Australia Pty Ltd. NCT04677933: A Study to Evaluate the Safety, Tolerability, Pharmacokinetics and Preliminary Efficacy of Multiple Subcutaneous Doses of OLP-1002. https://clinicaltrials.gov/ct2/show/NCT04677933 2020.

(29) Tawa, K.; Yao, D.; Knoll, W. Matching base-pair number dependence of the kinetics of DNA-DNA hybridization studied by surface plasmon fluorescence spectroscopy. *Biosens. Bioelectron.* **2005**, *21*, 322−329.

(30) Kambhampati, D.; Nielsen, P. E.; Knoll, W. Investigating the kinetics of DNA-DNA and PNA-DNA interactions using surface plasmon resonance-enhanced fluorescence spectroscopy. *Biosens. Bioelectron.* **2001**, *16*, 1109−1118.

(31) Persson, B.; et al. Analysis of Oligonucleotide Probe Affinities Using Surface Plasmon Resonance: A Means for Mutational Scanning. *Anal. Biochem.* **1997**, *246*, 34−44.

(32) Gotoh, M.; Hasegawa, Y.; Shinohara, Y.; Shimizu, M.; Tosu, M. A New Approach to Determine the Effect of Mismatches on Kinetic Parameters in DNA Hybridization Using an Optical Biosensor. *DNA Res.* **1995**, *2*, 285−293.

(33) Gidwani, V.; Riahi, R.; Zhang, D. D.; Wong, P. K. Hybridization kinetics of double-stranded DNA probes for rapid molecular analysis. *Analyst* **2009**, *134*, 1675−1681.

(34) Sassolas, A.; Leca-Bouvier, B. D.; Blum, L. J. DNA biosensors and microarrays. *Chem. Rev.* **2008**, *108*, 109−139.

(35) Marky, L. A.; Breslauer, K. J. Calculating Thermodynamic Data for Transitions of any Molecularity from Equilibrium Melting Curves. *Biopolymers* **1987**, *26*, 1601−1620.

(36) Andrews, R. DNA hybridisation kinetics using single-molecule fluorescence imaging. *Essays Biochem.* **2021**, *65*, 27−36.

(37) Ouldridge, T. E.; Šulc, P.; Romano, F.; Doye, J. P. K.; Louis, A. A. DNA hybridization kinetics: Zippering, internal displacement and sequence dependence. *Nucleic Acids Res.* **2013**, *41*, 8886−8895.

(38) Chung, S.; Jung, D.; Cho, B.; Jang, K.; Yoon, H. Androgen Receptor Antisense Oligonucleotides. *W.O. Patent No.* WO 2018/029517.

(39) Kilk, K.; Elmquist, A.; Saar, K.; Pooga, M.; Land, T.; Bartfai, T.; Soomets, U.; Langel, U. Targeting of antisense PNA oligomers to human galanin receptor type 1 mRNA. *Neuropeptides* **2004**, *38*, 316−324.

(40) Stein, J. A. C.; Ianeselli, A.; Braun, D. Kinetic Microscale Thermophoresis for Simultaneous Measurement of Binding Affinity and Kinetics. *Angew. Chem., Int. Ed.* **2021**, *60*, 13988−13995.

(41) Swenson, C. S.; Lackey, H. H.; Reece, E. J.; Harris, J. M.; Heemstra, J. M.; Peterson, E. M. Evaluating the effect of ionic strength on PNA:DNA duplex formation kinetics. *RSC Chem. Biol.* **2021**, *2*, 1249−1256.

(42) Xu, S.; Zhan, J.; Man, B.; Jiang, S.; Yue, W.; Gao, S.; Guo, C.; Liu, H.; Li, Z.; Wang, J.; Zhou, Y. Real-time reliable determination of

binding kinetics of DNA hybridization using a multi-channel graphene biosensor. *Nat. Commun.* **2017**, *8*, 14902.

(43) Yuan, B. F.; Zhuang, X. Y.; Hao, Y. H.; Tan, Z. Kinetics of base stacking-aided DNA hybridization. *Chem. Commun.* **2008**, *48*, 6600−6602.

(44) Glazer, R. W. Antigen-Antibody Binding and Mass Transport by Convection and Diffusion to a Surface: A Two-Dimensional Computer Model of Binding and Dissociation Kinetics. *Anal. Biochem.* **1993**, *213*, 152−161.

(45) Schuck, P.; Zhao, H. The role of mass transport limitation and surface heterogeneity in the biophysical characterization of macro-molecular binding processes by SPR biosensing. *Methods in molecular biology*; Clifton, N.J., 2010, *627*, 15−54.

(46) Vanjur, L.; Carzaniga, T.; Casiraghi, L.; Chiari, M.; Zanchetta, G.; Buscaglia, M. Non-Langmuir Kinetics of DNA Surface Hybrid-ization. *Biophys. J.* **2020**, *119*, 989−1001.

(47) De, A.; Souchelnytskyi, S.; van den Berg, A.; Carlen, E. T. Peptide nucleic acid (PNA)-DNA duplexes: Comparison of hybrid-ization affinity between vertically and horizontally tethered PNA probes. *ACS Appl. Mater. Interfaces* **2013**, *5*, 4607−4612.

(48) Jensen, K. K.; Ørum, H.; Nielsen, P. E.; Nordén, B. Kinetics for Hybridization of Peptide Nucleic Acids (PNA) with DNA and RNA Studied with the BIAcore Technique. *Biochemistry* **1997**, *36*, 5072−5077.

(49) Schwarz, F. P.; Robinson, S.; Butler, J. M. Thermodynamic comparison of PNA/DNA and DNA/ DNA hybridization reactions at ambient temperature. *Nucleic Acids Res.* **1999**, *27*, 4792−4800.

(50) Niranjani, G.; Murugan, R. Theory on the Mechanism of DNA Renaturation: Stochastic Nucleation and Zipping. *PLoS One* **2016**, *11*, No. e0153172.

(51) Ratilainen, T.; Holmén, A.; Tuite, E.; Nielsen, P. E.; Nordén, B. Thermodynamics of sequence-specific binding of PNA to DNA. *Biochemistry* **2000**, *39*, 7781−7791.

(52) Fiche, J. B.; Buhot, A.; Calemczuk, R.; Livache, T. Temperature effects on DNA chip experiments from surface plasmon resonance imaging: Isotherms and melting curves. *Biophys. J.* **2007**, *92*, 935−946.

(53) Sugimoto, N.; Satoh, N.; Yamamoto, K. Comparison of thermodynamic stabilities between PNA (peptide nucleic acid)/DNA hybrid duplexes and DNA/DNA duplexes. *Nucleic Acids Symp. Ser.* **1999**, *42*, 93−94.

(54) SantaLucia, J.; Allawi, H. T.; Seneviratne, P. A. Improved nearest-neighbor parameters for predicting DNA duplex stability. *Biochemistry* **1996**, *35*, 3555−3562.

(55) SantaLucia, J., Jr.; Hicks, D. The thermodynamics of DNA structural motifs. *Annu. Rev. Biophys. Biomol. Struct.* **2004**, *33*, 415−440.

(56) Zhou, H. X.; Pang, X. Electrostatic Interactions in Protein Structure, Folding, Binding, and Condensation. *Chem. Rev.* **2018**, *118*, 1691−1741.